

1
2
3
4
5
6
7
8
9 **HuR Thermal Stability is dependent on Domain Binding and upon**
10 **Phosphorylation**
11
12
13
14
15
16

17 **Rafael Manfred Scheiba, Ángeles Aroca and Irene Díaz-Moreno***
18
19
20
21

22 Instituto de Bioquímica Vegetal y Fotosíntesis, cicCartuja, Universidad de Sevilla-
23
24 CSIC, Americo Vespucio 49, Sevilla 41092, Spain
25
26
27
28
29
30

31
32 **Running head:** Thermal Stability of HuR
33
34
35
36

37 **Address correspondence to:**
38

39 Irene Díaz-Moreno
40

41
42 Telephone: +34 954489513; Fax: +34 954460065; Email: idiuzmoreno@us.es
43
44
45
46
47
48
49
50
51
52
53
54
55
56
57
58
59
60
61
62
63
64
65

1
2 **Abstract**
3

4 Human antigen R (HuR) is a multitasking RNA binding protein involved in post-
5 transcriptional regulation by recognizing Adenine and uracile Rich Elements (AREs)
6 placed at the 3' untranslated regions of mRNAs. The modular architecture of the
7 protein, which consists of two N-terminal RNA recognition motifs (RRMs) in tandem
8 spaced from a third one by a nuclear-cytoplasmic shuttling sequence, controls stability
9 of many mRNA targets, as well as their translation rates. A higher level of regulation
10 comes from the fact that both localization and function of HuR is strictly regulated by
11 phosphorylation. Here, we report how the thermal stability of RRM2 is decreased by the
12 presence of RRM1, indicating that both domains are interacting in solution. In addition,
13 even though no significant structural changes are observed among mutants of HuR
14 RRM12 mimicking phosphorylated species, slight differences in stability are
15 appreciable, which may explain the RNA binding activity of HuR.
16
17
18
19
20
21
22
23
24
25
26
27
28
29
30
31
32
33
34
35
36
37
38
39
40
41
42
43
44

45 **Keywords:**

46 HuR; Phosphorylation; Post-translational Modifications; RNA Binding Protein; RNA
47
48 Recognition Motif; Protein Thermal Stability.
49
50
51
52
53
54
55
56
57
58
59
60
61
62
63
64
65

Abbreviations:

1
2 AREs: Adenine and uracile Rich Elements
3

4 CARM1: Coactivator-associated ARginine Methyltransferase 1 protein
5
6

7 CD: Circular Dichroism
8

9 Chk2: Checkpoint 2 kinase
10

11 Cdk: Cycline dependent kinase 1
12

13 DSF: Differential Scanning Fluorimetry
14

15 DTT: DiThioThreitol
16

17 ELAV: Embryonic Lethal and Abnormal Vision
18

19 HNS: Human Novel Shuttling
20

21 HuR: Human antigen R
22

23 HuR FL: HuR full-length
24

25 K_D : Dissociation affinity constant
26

27 PKC α : Protein Kinase C α
28

29 PKC δ : Protein Kinase C δ
30

31 RBP: RNA Binding Protein
32

33 RMSD: Root Mean Square Deviation
34

35 RRM: RNA Recognition Motif
36

37 RRM12 WT: RRM12 *wild-type*
38

39 RT-PCR: Real Time Polymerase Chain Reaction
40

41 T_m : Midpoint Melting Temperature
42

43 UTRs: UnTranslated Regions
44
45
46
47
48
49
50
51
52
53
54
55
56
57
58
59
60
61
62
63
64
65

Introduction

Human antigen R (HuR) is a ubiquitous 36-kDa RNA Binding Protein (RBP) consisting of three RNA Recognition Motifs (RRMs; Birney et al. 1993; Ma et al. 1996). HuR (also known as ELAV-like protein 1) plays a key role in cell cycle, stress stimuli, inflammation and cancer. HuR controls such functions by recognizing the Adenine and uracil Rich Elements (AREs) placed at the 3'-Untranslated Regions (UTRs) of certain RNA (Abdelmohsen et al. 2007a; Brennan et al. 2001; Dixon et al. 2001; Gorospe 2003; Sengupta et al. 2003). As a consequence, the expression level of these RNA targets is affected, so dependent processes in the cell are regulated. In fact, HuR has been characterized as an anti-apoptotic switch tightly regulated by a post-transcriptional orchestration (Abdelmohsen et al. 2007a). However, it has been recently reported that pro-apoptotic reactions can also be supported, which depend on the caspase-mediated cleavage of HuR (Mazroui et al. 2008).

It is worth to mention that there are many studies concerning the behavior of HuR in the cellular environment, although little is known about the structure and the related molecular mechanisms of this RBP. HuR is a multidomain protein whose three RRMs show the canonical topology: $\beta_1\alpha_1\beta_2\beta_3\alpha_2\beta_4$. Interestingly, the most N-terminal RRM domains – named RRM1 and RRM2 - are in tandem only separated by a 3_{10} -helix turn, whereas the C-terminal RRM3 motif is spaced by a 60-residue linker spanning the hinge called Human Novel Shuttling (HNS) sequence (Figure 1a; Fan et al. 1998). Actually, HNS is known to determine the cellular localization of HuR either in the nucleus or the cytoplasm. Recently, the crystal structure of the first N-terminal RRM domain has been solved (Benoit et al. 2010), although the global protein structure remains unknown.

Post-translational modifications play an essential role in the cellular function of HuR. Recent research has revealed several phosphorylation sites in HuR which

1 influence the interaction with its RNA targets, with other proteins and even in its
2 cellular localization (Abdelmohsen et al. 2007b; Doller et al. 2008; Kim et al. 2008a-c).
3
4 Such phosphorylations can be performed by different kinases as Checkpoint 2 kinase
5 (Chk2), Cycline-dependent kinase 1 (Cdk1) and Protein Kinases C α or δ (PKC α or
6 PKC δ). Upon HuR phosphorylation, different cellular responses have been described
7 (Abdelmohsen, 2007 a,b; Doller et al. 2008; Kim 2008a-c). Whereas the HuR capability
8 for binding to RNA targets increases or decreases when Chk2 phosphorylates HuR at
9 Ser88 or Ser100 residues, respectively (Abdelmohsen et al. 2007b), the addition of a
10 phosphate group to Ser158, Ser221 and Ser318 by PKC favors the cytoplasmic
11 localization of HuR instead of the preferred nuclear localization of the protein (Doller et
12 al. 2008, 2009), along with an enhancement in the mRNA binding (Doller et al. 2007).
13
14 In addition to Ser221 at HNS, HuR also becomes phosphorylated at Ser242, which is
15 also involved in the nucleocytoplasmic shuttling (Kim et al. 2008c). The HuR shuttling
16 can provide information about the cell state. Indeed, an increase of cytoplasmic HuR
17 levels is an indicator for the stress response of the cell (Gorospe, 2003) or different kind
18 of cancer diseases (Denkert et al. 2004; Heinonen et al. 2005).
19
20
21
22
23
24
25
26
27
28
29
30
31
32
33
34
35
36
37
38

39 An additional HuR post-translational modification consists on a methylation at
40 Arg117 by CARM1 (Coactivator-associated ARginine Methyltransferase 1) protein (Li
41 et al. 2002).
42
43
44
45

46 Given that both functionality and localization of HuR are strictly regulated by
47 phosphorylation, exploring the stability of its N-terminal RRM domains after being
48 post-translationally modified would be highly valuable to understand the pleiotropic
49 role of HuR in mRNA metabolism. Within this frame, this work suggests that the
50 domains RRM1 and RRM2 as a cooperative assembly remains unchanged upon
51 phosphorylation events of three Ser residues localized inside RRM motifs (the non-
52 conserved Ser88 and Ser158 at RRM1 and RRM2, respectively) and at the interdomain
53
54
55
56
57
58
59
60
61
62
63
64
65

linker (Ser100 highly conserved among the family members HuB, HuC and HuD, as well as the ELAV - Embryonic Lethal and Abnormal Vision - *Drosophila* homologue).

1
2
3
4
5
6
7
8
9
10
11
12
13
14
15
16
17
18
19
20
21
22
23
24
25
26
27
28
29
30
31
32
33
34
35
36
37
38
39
40
41
42
43
44
45
46
47
48
49
50
51
52
53
54
55
56
57
58
59
60
61
62
63
64
65

Materials and Methods

Site-Directed Mutagenesis of HuR RRM Constructs

pGEX 5X2 vectors containing the sequences coding for HuR *full-length* (HuR FL) as well as individual N-terminal RRM domains – RRM1 and RRM2 - and the two-domain construct RRM12, have been kindly provided by Dr. M. Gorospe (*National Institute of Health, Baltimore, USA*) and Dr. J.A. Steitz (*Yale University, New Haven, USA*). These genes were further cloned into the pGEX-4T2 vector, which was modified for RRM12 and HuR FL as follows: The GST sequence was substituted by a 6xHis-tag using the following primers: 5′ CATCATCACCACCATCACctggttccgcgtggatccccagg 3′ (forward primer) and 5′ GTGATGGTGGTGATGATGcatgaatactgttctctgttg 3′ (reverse primer) to facilitate the purification. Both GST and 6xHis tags were cleaved with thrombine, resulting in a short additional aminoacid sequence for all constructs “GSPGIPSNYEDH”, with a negligible effect on the secondary structure analysis. Serines at positions 88, 100 and 158 of the RRM12 construct were replaced by alanines or aspartates by site-directed mutagenesis (Mutagenex, Piscataway, USA).

Protein Expression and Purification of HuR Constructs

Recombinant proteins were expressed in *E. coli* BL21-T1^R (SIGMA, St. Louis, USA) cells as follows. Competent cells were transformed with plasmid DNA and were grown at 30 °C for HuR FL and at 37 °C for RRM1, RRM2 and RRM12 constructs, both in LB medium supplemented with ampicillin (50 µg/ml). Protein expression was induced by the addition of 1 mM IPTG once the culture reached an O.D.₆₀₀ of 0.6–0.8. After 5 h expression in LB medium at 30 °C for HuR FL and at 37 °C for the other constructs, cells were harvested by centrifugation at 7000 g and further resuspended in 50 mM Tris Buffer (pH 8.0) for its storage at -80 °C. The HuR FL protein was resuspended in the same buffer but supplemented with 800 mM NaCl.

1 GST fusion proteins were purified using a Glutathione Sepharose High
2 Performance Matrix (GE Healthcare, Piscataway, USA), whereas His-tagged constructs
3 were purified by nickel affinity chromatography (Ni Sepharose™ Fast Flow Matrix, GE
4 Healthcare, Piscataway, USA). All constructs were expressed with thrombine-cleavable
5 GST or His tags (GE Healthcare, Piscataway, USA). To separate HuR RRM single
6 domains from the cleaved GST protein, a gel filtration chromatography (sephadex G-75
7 matrix; SIGMA, St. Louis, USA) was performed.

8
9
10
11
12
13
14
15
16
17 Samples were concentrated to 80 μ M in 10 mM sodium phosphate (pH 7.3) with
18 0.5 mM DTT. HuR FL was supplemented with 800 mM of NaCl and 0.1% of Sarkosyl
19 detergent to increase its solubility during all purification steps. Protein concentration
20 was determined using spectrophotometry with predicted extinction coefficients. All
21 molecular weights of the HuR constructs used in this work were verified by MALDI-
22 TOF spectroscopy.

33 34 **Circular Dichroism Spectroscopy**

35
36 All Circular Dichroism (CD) spectra were recorded in the far-UV range (190–
37 250 nm) at 298 K on a Jasco J-815 spectropolarimeter, equipped with a Peltier
38 temperature-control system, using a 1-mm quartz cuvette. Protein concentration was 12
39 μ M in 10 mM sodium phosphate buffer (pH 7.3) supplemented with 0.5 mM DTT. For
40 each sample, 20 scans were averaged for further secondary structure analysis using
41 CDPRO software (Sreerama et al. 2000), which includes the algorithms CONTIN,
42 SELCON and CDSSTR, as well as the CLSTR option to compare with a set of proteins
43 with similar folds.

44
45
46
47
48
49
50
51
52
53
54
55
56 Thermal unfolding experiments were carried out in a range of temperatures from
57 298 K to 371 K. For all these assays, the HuR species at 12 μ M final concentration were
58 dissolved in 10 mM sodium phosphate (pH 7.3) with 0.5 mM DTT. Temperature was
59
60
61
62

1 increased at a rate of 1 K per min with an error within ± 0.1 K. Spectra were recorded at
2 the scan rate, band width and sensitivity of 200 nm min⁻¹, 1.0 nm and 0.2 deg,
3
4 respectively. Protein unfolding was monitored by recording the CD signal at 195, 208
5
6 and 235 nm. The experimental data were fitted to a two-state native-denatured model
7
8
9 (Privalov 1979).
10

11 RNA binding was monitored by adding increasing amounts of protein to 4 μ M
12
13 AU-11mer (AUUUUUAUUUU) RNA in 10 mM sodium phosphate pH 7.3, 0.5 mM
14
15 DTT solution. A temperature of 298 K was chosen to optimize the signal change upon
16
17 protein binding. Each CD spectrum was the average of 10 scans. The integral of this
18
19 averaged signal between 260 and 275 nm was fitted against the protein concentration
20
21 according to Santoro and Bolen (Santoro and Bolen, 1988).
22
23
24
25
26
27

28 **Diferential Scanning Fluorimetry**

29 Thermal unfolding of HuR constructs was monitored by Differential Scanning
30
31 Fluorimetry (DSF), in the presence of the fluorescent SYPRO Orange dye (Invitrogen,
32
33 Carlsbad, CA, USA), by using an IQ5 Multicolor Real-Time PCR Detection Instrument
34
35 (BioRad; Niesen et al. 2007). The commercial dye (5000 \times concentrate in DMSO) was
36
37 at least ten-fold diluted in 10 mM sodium phosphate buffer (pH 7.3), supplemented with
38
39 0.5 mM DTT, and the HuR samples (10-40 μ g protein) were added at 25 μ L final
40
41 volume. The thermal unfolding process was monitored between 293 K and 369 K,
42
43 increasing the temperature at a rate of 1 K per min. The values for the midpoint melting
44
45 temperature (T_m) were calculated from the first derivative in Origin 8.0 (Microcal Inc.)
46
47 and a non linear curve fitting function was used (Privalov, 1979).
48
49
50
51
52
53
54
55
56
57
58
59
60
61
62
63
64
65

Results

HuR RRM Domains Adopt a Canonical Topology with Negligible Changes in their Secondary Structure upon Phosphorylation

The crystallographic structure of HuR RRM1 – recently published by Benoit et al. 2010 - shows the canonical RRM folding adopting the $\beta\alpha\beta\beta\alpha\beta$ topology.

We have obtained a homology model of HuR RRM12 construct (Figure 1b and 1c) using the crystallographic structure of its homologue HuD RRM12 as a template (PDB entry 1FXL; Wang et al. 2001). Sequence identity to the target was 75.4 % and the model was built with the SWISS-MODEL server (Arnold et al. 2006; Kiefer et al. 2009) and graphically represented using Chimera software (Pettersen et al. 2004). Figure 1c shows the superposition of both HuR structures: the homology model of RRM12 and the crystallographic structure of RRM1.

Our homology model is in a good agreement with the secondary structure contents for HuR constructs. Figure 2 shows the normalized far-UV CD spectra of isolated RRM1 and RRM2 domains, the tandem RRM12 and the HuR FL protein. Notably, all HuR species show similar global secondary structures with minor differences, as summarized in Table 1. Whereas all constructs share similar β -strand and turns contents, RRM2 differs from RRM1 and RRM12 in its higher α -helix content.

RRM12 mutants, in which Ser88, Ser100 and Ser158 have been substituted by aspartic acid residues to mimic phosphorylation events, exhibit secondary structure as that of RRM12 *wild-type* (RRM12 WT). In addition, Ser-by-Ala control mutations show similar CD spectra (Figure 3 and Table 1).

For further thermal stability on RRM12 WT and its mutants, the impact of Cys13 in the homodimer formation needs to be evaluated (Meisner et al., 2007; Benoit et al., 2010). Figure 4 shows an SDS-page gel of RRM12 WT in absence and in presence of DiThioThreitol (DTT) at 0.5 and 5 mM, as reducing agent. RRM12 WT is

1 clearly a monomer upon DTT addition, albeit the monomer-dimer equilibrium appears
2 in samples devoid of DTT. This data are recently confirmed by analytical
3 ultracentrifugation on RRM12 WT samples containing 0.5 mM DTT (data not shown).
4 Thus, RRM12 WT construct, which includes Cys13, behaves as a monomer, at least in
5 the experimental conditions used in this work.
6
7
8
9
10

11 **Thermal stability of HuR RRM2 is decreased by the presence of RRM1**

12
13
14
15
16
17 Recently, it has been demonstrated that the thermal stability of RNA binding
18 domains reveals interactions between neighboring modules (Aroca et al. 2011; Díaz-
19 Moreno et al. 2010). Thermal unfolding studies on the single N-terminal RRM
20 segments and the two-domain construct from HuR were performed in order to confirm
21 the assembly between RRM1 and RRM2, as inferred from the homology model of HuR
22 RRM12 and the crystal structure of HuD RRM12 (Wang et al. 2001). CD spectroscopy
23 shows that the T_m for isolated RRM1 (335 ± 3 K) is lower than the one for RRM2 (341
24 ± 2 K; Table 2). Interestingly, RRM12 is as stable as RRM1 (335 ± 2 K) suggesting
25 that inter-domain interactions are taking place. Such interaction lowers the T_m of RRM2
26 in ca. 6 K, as previously reported for other RNA binding proteins (Aroca et al. 2011;
27 Díaz-Moreno et al. 2010). In addition, the denaturation curve of RRM12 is not the sum
28 of the denaturation curves of the two individual RRM1 and RRM2 domains, revealing
29 that only one transition state is observed (not two). Indeed, the cooperativity of the
30 RRM12 denaturation is strongly reduced as compared with that of the individual
31 domains.
32
33
34
35
36
37
38
39
40
41
42
43
44
45
46
47
48
49
50
51

52
53 These changes in stability between isolated RRM2 and RRM2 in RRM12
54 construct are confirmed by DSF although ΔT_m is somewhat slightly higher (7 K; Table 2
55 and Figure 5a). Intriguingly, T_m values calculated by DSF for HuR species are always
56
57
58
59
60
61
62
63
64
65

1 equal or lower than those estimated by CD, although ΔT_m is quite independent of the
2 technique used (see Table 2).
3
4
5
6

7 **Stability of HuR RRM12 is Regulated by Phosphorylation**

8
9 To analyze the phosphorylation effect of serine residues on the stability of HuR
10 RRM12 construct, this post-translational modification has been mimicked by Ser-to-
11 Asp substitutions. Even though the use of Ser/Asp mutations simulates a constitutively
12 phosphorylated protein with only one negative charge, it is herein extensively
13 recommended since two out of three serine residues of RRM12 WT – those at positions
14 88 and 100 - become phosphorylated by the same kinase, Chk2, being *in vitro* kinase
15 assays undesirable.
16
17
18
19
20
21
22
23
24
25

26 The non-conserved serine residues, which are localized inside the RRM core,
27 play an essential role in the stability of HuR RRM12. It is worth to mention that
28 phosphorylation at Ser88 in RRM1 mimicked by the S88D mutant makes the RRM12
29 construct slightly more stable than its control mutant (S88A) and RRM12 WT. Indeed,
30 T_m of RRM12 S88D is increased in more than 5 K, using both CD and DSF approaches
31 (Table 2 and Figure 5b). In contrast, the addition of a negatively-charged group at
32 position 158 (mutation S158D) slightly destabilizes HuR RRM12 with regard to the
33 S158A mutant and RRM12 WT, despite the discrepancies on ΔT_m between CD and
34 DSF. The well-conserved Ser100, which takes part of the short linker between RRM1
35 and RRM2, displays no significant contributions in thermal stability of HuR RRM12
36 upon mutations ($\Delta T_m < 2.0$ K). As expected, the non-phosphorylatable Ser-to-Ala
37 RRM12 mutants behave as RRM12 WT in terms of thermal stability, suggesting that
38 HuR phosphorylation has functional consequences rather than structural effects.
39
40
41
42
43
44
45
46
47
48
49
50
51
52
53
54
55
56
57
58
59
60
61
62
63
64
65

RNA binding of HuR RRM12 is Regulated by Phosphorylation

1
2
3
4
5
6
7
8
9
10
11
12
13
14
15
16
17
18
19
20
21
22
23
24
25
26
27
28
29
30
31
32
33
34
35
36
37
38
39
40
41
42
43
44
45
46
47
48
49
50
51
52
53
54
55
56
57
58
59
60
61
62
63
64
65

To understand how the interaction of HuR-RRM12 with *c-fos* AU-11 mer RNA may be regulated upon phosphorylation, we assessed the affinity of RRM12 WT and its phosphomimetic mutants for the RNA target and explored whether the phosphorylation could modulate recognition *in vitro*, similarly than *in vivo*. We used CD to obtain quantitative data over affinities which lie in the μM range. Our CD data show that the affinity of the two RRM1 and RRM2 domains for the RNA is in the low micromolar range ($2.6 \pm 0.2 \mu\text{M}$; Table 3 and Figure 6). Next, we investigated the effect of phosphorylation at RRM1 and at the RRM12 linker by RRM12 S88D and RRM12 S100D mutants, respectively, which show K_D values comparable with that of RRM12 WT ($2.7 \pm 0.2 \mu\text{M}$ for S88D and $2.0 \pm 0.1 \mu\text{M}$ for S100D; Table 3). In contrast, RRM12 S158D favors RNA binding ($0.6 \pm 0.3 \mu\text{M}$; Table 3) in agreement what has been previously published *in vivo* (Doller *et al.*, 2007).

Discussion

1
2
3
4
5
6
7
8
9
10
11
12
13
14
15
16
17
18
19
20
21
22
23
24
25
26
27
28
29
30
31
32
33
34
35
36
37
38
39
40
41
42
43
44
45
46
47
48
49
50
51
52
53
54
55
56
57
58
59
60
61
62
63
64
65

HuR consists of three RRM domains, whose function in RNA binding is well-characterized, despite the global function and working mechanisms of HuR FL protein are still not fully understood. The interaction between RRM1 and RRM2 as a tandem construct shows the meaning of the modules and the role of binding to each other. The combination of the individual RRM domains with additional post-translational modification sites enables a high variety of regulation of HuR. With the possibility of being phosphorylated (Kim et al. 2008a-c), methylated (Li et al. 2002), ubiquitinated (Abdelmohsen et al. 2009), submitted to protease cleavage mechanism (Mazroui et al. 2008) and recently neddylated (Embade et al. 2011), HuR has a huge probability of changing its cellular localization, the binding to other proteins and RNA processing.

Thermal stability studies on HuR species indicate the importance of the cooperation between the the two N-terminal RRM domains of HuR, which work as a functional unit. The comparison of T_m values for isolated RRM1 or RRM2 and the two-domain construct RRM12 reveals that RRM12 shows the same thermal stability as RRM1, while RRM2 is substantially more stable. In addition, the fact that the denaturation curve of HuR RRM12 is not the sum of those from the two individual RRM1 and RRM2 domains suggest cooperativity between both modules.

It is tempting to speculate that the RRM12 modular interaction is essential for RNA recognition activity, similarly to what previously observed for RRM1-RRM2 motifs of the homologous HuD protein upon *c-fos* RNA binding (Wang et al. 2001). Indeed, the preferred orientation between RNA binding domains helps to establish a high-affinity RNA-binding platform (Vitali et al. 2006; Li et al. 2010) and/or to stabilize a suitable conformation that can adapt to the changes in the direction of the RNA chain inside the highly structured 3' UTRs, as previously suggested (Díaz-Moreno et al. 2010).

1
2
3
4
5
6
7
8
9
10
11
12
13
14
15
16
17
18
19
20
21
22
23
24
25
26
27
28
29
30
31
32
33
34
35
36
37
38
39
40
41
42
43
44
45
46
47
48
49
50
51
52
53
54
55
56
57
58
59
60
61
62
63
64
65

To study changes in structure and stability of HuR induced by serine phosphorylation, we have designed three Ser-by-Asp mutations. Two of them are localized at the RRM cores, while the third one is in the inter-domain linker. For none of these phosphomimetic mutants significant changes in secondary structure were observed, unlike what has been recently published for other RNA binding domains (Díaz-Moreno et al. 2009). Therefore, phosphorylation effects on HuR seem to be essentially related to RNA binding properties and/or intermolecular protein interactions than to changes on the HuR structure, as confirmed our CD RNA binding titrations (Figure 6).

22
23
24
25
26
27
28
29
30
31
32
33
34
35
36
37
38
39
40
41
42
43
44
45
46
47
48
49
50
51
52
53
54
55
56
57
58
59
60
61
62
63
64
65

Nevertheless the thermal stability of HuR constructs is regulated by phosphorylation. The phosphomimetic mutant S88D slightly stabilizes RRM1 in the RRM12 context, which can be explained by the addition of a negative charge into the protein loop mainly governed by two positively charged residues (Benoit et al. 2010). Thus, Asp88 could minimize the electrostatic repulsion between Arg85 and Lys89, which would restrict the loop mobility. In terms of RNA binding, it has been previously reported that *in vivo* HuR phosphorylation at Ser88 increases the docking of RNA targets to the RNA binding sites (Abdelmohsen et al. 2007b). Also it is proposed that the phosphoserine at position 88 makes a Mg²⁺-ion-mediated interaction with a phosphate group from RNA (Benoit et al. 2010). However, no substantial differences in binding affinities were observed between RRM12 WT and the phosphomimetic RRM12 S88D mutant by performing *in vitro* CD titrations using *c-fos*-RNA.

51
52
53
54
55
56
57
58
59
60
61
62
63
64
65

Slightly destabilizing phosphorylation of Ser158 could be explained based on electrostatic repulsion with another nearby negative residue Glu162, although the negatively-charged Asp158 is added at the N-end of helix α_2 of HuR RRM2. Post-translational modification of Ser158 at RRM2 domain – mimicked by the RRM12 S158D mutation – tightly regulates the binding of HuR RRM12 with *c-fos* RNA *in*

1
2
3
4
5
6
7
8
9
10
11
12
13
14
15
16
17
18
19
20
21
22
23
24
25
26
27
28
29
30
31
32
33
34
35
36
37
38
39
40
41
42
43
44
45
46
47
48
49
50
51
52
53
54
55
56
57
58
59
60
61
62
63
64
65

vitro. Actually, the RNA binding affinity of RRM12 S158D is four times larger than the one of RRM12 WT, in agreement with previous data *in vivo* (Doller et al. 2007). Phosphorylation at the level on the RRM12 linker region – Ser100 – has also a negligible effect on HuR stability. A plausible explanation is that this solvent-exposed residue does not make many contacts with neighbors. Intriguingly, phosphorylation at Ser100 increases RNA binding *in vivo* (Abdelmohsen et al. 2007b), although the equivalent serine in the homologous HuD – Ser126 - is facing away from the RNA in the HuD/*c-fos* mRNA crystal structure (Wang et al. 2001). *In vitro* CD titrations reveal no effect of the S100D mutation on RNA recognition with respect to RRM12 WT. *in vitro* Therefore, phosphorylation at this site would influence RRM2–interdomain linker interactions and the rearrangement between RRM domains, rather than directly repulsing RNA (Benoit et al. 2010).

Perturbations in stability of HuR upon post-translational modifications such as phosphorylation may explain the HuR behavior in binding RNA molecules, as well as in determining their lifetime and translation rate.

Acknowledgements

The authors wish to thank Dr. M. Gorospe (NIH, Baltimore, USA) and Dr. J.A. Steitz (Yale University, New Haven, USA) for providing the HuR vectors. We are grateful to Prof. Miguel A. De la Rosa and Dr. Antonio Díaz-Quintana for critical reading of the manuscript. For financial support we thank the Andalusian Government (P07-CVI-02896) and the Spanish Scientific Council Fellowship (JAEpre_08_00375).

References

- 1
2
3 Abdelmohsen K, Lal A, Kim HH, Gorospe M (2007a) Posttranscriptional orchestration
4
5 of an anti-apoptotic program by HuR. *Cell Cycle* 6:1288–1292
6
7
8
9 Abdelmohsen K, Pullmann RJr, Lal A, Kim HH, Galban S, Yang X, Blethrow JD,
10
11 Walker M, Shubert J, Gillespie DA, Furneaux H, Gorospe M (2007b) Phosphorylation
12
13 of HuR by Chk2 regulates SIRT1 expression. *Mol Cell* 25:543–557
14
15
16
17 Abdelmohsen K, Srikantan S, Yang X, Lal A, Kim HH, Kuwano Y, Galban S, Becker
18
19 KG, Kamara D, de Cabo R, Gorospe M (2009) Ubiquitin-mediated proteolysis of HuR
20
21 by heat shock. *EMBO J* 28:1271–1282
22
23
24
25 Arnold K, Bordoli L, Kopp J, Schwede T (2006) The SWISS-MODEL Workspace: A
26
27 web-based environment for protein structure homology modelling. *Bioinformatics*
28
29 22:195–201
30
31
32
33 Aroca A, Díaz-Quintana A, Díaz-Moreno I (2011) A structural insight into the C-
34
35 terminal RNA recognition motifs of T-cell intracellular antigen-1 protein. *FEBS Lett*
36
37 585:2958–2964
38
39
40
41
42 Benoit RM, Meisner NC, Kallen J, Graff P, Hemmig R, Cebe R, Ostermeier C, Widmer
43
44 H, Auer M (2010) The x-ray crystal structure of the first RNA recognition motif and
45
46 site-directed mutagenesis suggest a possible HuR redox sensing mechanism. *J Mol Biol*
47
48 397:1231–1244
49
50
51
52
53 Birney E, Kumar S, Krainer AR (1993) Analysis of the RNA-recognition motif and RS
54
55 and RGG domains: conservation in metazoan pre-mRNA splicing factors. *Nucleic*
56
57 *Acids Res* 21:5803–5816
58
59
60
61 Brennan CM, Steitz JA (2001) HuR and mRNA stability. *Cell Mol Life Sci* 58:266–277
62
63
64
65

1 Denkert C, Weichert W, Winzer KJ, Muller BM, Noske A, Niesporek S, Kristiansen G,
2 Guski H, Dietel M, Hauptmann S (2004) Expression of the ELAV-like protein HuR is
3 associated with higher tumor grade and increased cyclooxygenase-2 expression in
4 human breast carcinoma. *Clin Cancer Res* 10:5580–5586
5
6
7

8
9
10 Díaz-Moreno I, Hollingworth D, Frenkiel TA, Kelly G, Martin S, Howell S, García-
11 Mayoral M, Gherzi R, Briata P, Ramos A (2009) Phosphorylation-mediated unfolding
12 of a KH domain regulates KSRP localization via 14-3-3 binding. *Nat Struct Mol Biol*
13 16:238–246
14
15
16
17

18
19
20 Díaz-Moreno I, Hollingworth D, Kelly G, Martin S, García-Mayoral M, Briata P,
21 Gherzi R, Ramos A (2010) Orientation of the central domains of KSRP and its
22 implications for the interaction with the RNA targets. *Nucleic Acids Res* 38:5193–5205
23
24
25
26

27
28
29 Dixon DA, Tolley ND, King PH, Nabors LB, McIntyre TM, Zimmerman GA, Prescott
30 SM (2001) Altered expression of the mRNA stability factor HuR promotes
31 cyclooxygenase-2 expression in colon cancer cells. *J Clin Invest* 108:1657–1665
32
33
34
35

36
37
38 Doller A, Huwiler A, Muller R, Radeke HH, Pfeilschifter J, Eberhardt W (2007) Protein
39 kinase C alpha-dependent phosphorylation of the mRNA-stabilizing factor HuR:
40 implications for posttranscriptional regulation of cyclooxygenase-2. *Mol Biol Cell*
41 18:2137–2148
42
43
44
45

46
47
48 Doller A, Pfeilschifter J, Eberhardt W (2008) Signalling pathways regulating nucleo-
49 cytoplasmic shuttling of the mRNA-binding protein HuR. *Cell Signal* 20:2165–2173
50
51
52

53
54
55 Doller A, Schlepckow K, Schwalbe H, Pfeilschifter J, Eberhardt W (2009) Tandem
56 phosphorylation of serines 221 and 318 by protein kinase Cdelta coordinates mRNA
57 binding and nucleocytoplasmic shuttling of HuR. *Mol Cell Biol* 30:1397–1410
58
59
60
61

1 Embade N, Fernández-Ramos D, Varela-Rey M, Beraza N, Sini M, de Juan VG,
2 Woodhoo A, Martínez-López N, Rodríguez-Iruretagoyena B, Bustamante FJ, de la Hoz
3 AB, Carracedo A, Xirodimas DP, Rodríguez MS, Lu SC, Mato JM, Martínez-Chantar
4 ML (2011) Mdm2 regulates HuR stability in human liver and colon cancer through
5 neddylation. *Hepatology* doi: 10.1002/hep.24795
6
7
8
9
10
11
12 Fan XC, Steitz JA (1998) HNS, a nuclear-cytoplasmic shuttling sequence in HuR. *Proc*
13 *Natl Acad Sci U S A* 95:15293–15298
14
15
16
17
18
19 Gorospe M (2003) HuR in the mammalian genotoxic response: post-transcriptional
20 multitasking. *Cell Cycle* 2:412–414
21
22
23
24
25 Kiefer F, Arnold K, Künzli M, Bordoli L, Schwede T (2009) The SWISS-MODEL
26 Repository and associated resources. *Nucleic Acids Res* 37:D387–D392
27
28
29
30
31 Kim HH, Abdelmohsen K, Lal A, Pullmann RJr, Yang X, Galban S, Srikantan S,
32 Martindale JL, Blethrow J, Shokat KM, Gorospe M (2008a) Nuclear HuR accumulation
33 through phosphorylation by Cdk1. *Genes Dev* 22:1804–1815
34
35
36
37
38
39 Kim HH, Gorospe M (2008b) Phosphorylated HuR shuttles in cycles. *Cell Cycle*
40 7:3124–3126
41
42
43
44
45 Kim HH, Yang X, Kuwano Y, Gorospe M (2008c) Modification at HuR(S242) alters
46 HuR localization and proliferative influence. *Cell Cycle* 21:3371–3377
47
48
49
50
51 Heinonen M, Bono P, Narko K, Chang SH, Lundin J, Joensuu H, Furneaux H, Hla T,
52 Haglund C, Ristimaki A (2005) Cytoplasmic HuR expression is a prognostic factor in
53
54
55
56
57
58
59
60
61
62
63
64
65

1
2
3
4
5
6
7
8
9
10
11
12
13
14
15
16
17
18
19
20
21
22
23
24
25
26
27
28
29
30
31
32
33
34
35
36
37
38
39
40
41
42
43
44
45
46
47
48
49
50
51
52
53
54
55
56
57
58
59
60
61
62
63
64
65

Li H, Park S, Kilburn B, Jelinek MA, Henschen-Edman A, Aswad DW, Stallcup MR, Laird-Offringa IA (2002) Lipopolysaccharide-induced methylation of HuR, an mRNA-stabilizing protein, by CARM1. Coactivator-associated arginine methyltransferase. *J Biol Chem* 277:44623–44630

Li H, Shi H, Wang H, Zhu Z, Li X, Gao Y, Cui Y, Niu L, Teng M (2010) Crystal structure of the two N-terminal RRM domains of Pub1 and the poly(U)-binding properties of Pub1. *J Struct Biol* 171:291–297

Ma WJ, Cheng S, Campbell C, Wright A, Furneaux H (1996) Cloning and characterization of HuR, a ubiquitously expressed Elav-like protein. *J Biol Chem* 271:8144–8151

Mazroui R, Di Marco S, Clair E, von Roretz C, Tenenbaum SA, Keene JD, Saleh M, Gallouzi IE (2008) Caspase-mediated cleavage of HuR in the cytoplasm contributes to pp32/PHAP-I regulation of apoptosis. *J Cell Biol* 180:113–127

Meisner NC, Hintersteiner M, Mueller K, Bauer R, Seifert JM, Naegeli HU, Ottl J, Oberer L, Guenat C, Moss S, Harrer N, Woisetschlaeger M, Buehler C, Uhl V, Auer M (2007) Identification and mechanistic characterization of low-molecular-weight inhibitors for HuR. *Nat Chem Biol* 3:508–515

Niesen FH, Berglund H, Vedadi M (2007) The use of differential scanning fluorimetry to detect ligand interactions that promote protein stability. *Nat Protoc* 2:2212–2221

Pettersen EF, Goddard TD, Huang CC, Couch GS, Greenblatt DM, Meng EC, Ferrin TE (2004) UCSF Chimera - a visualization system for exploratory research and analysis. *J Comput Chem* 25:1605–1612

1 Privalov PL (1979) Stability of proteins: small globular proteins. *Adv Protein Chem*
2 33:167–241
3

4
5 Santoro MM, Bolen DW (1988) Unfolding free energy changes determined by the
6 linear extrapolation method. 1. Unfolding of phenylmethanesulfonyl alpha-
7 chymotrypsin using different denaturants. *Biochemistry* 27:8063–8068
8
9

10
11 Sengupta S, Jang BC, Wu MT, Paik JH, Furneaux H, Hla T (2003) The RNA-binding
12 protein HuR regulates the expression of cyclooxygenase-2. *J Biol Chem* 278:25227–
13 25233
14
15

16
17 Sreerama N, Woody RW (2000) Estimation of protein secondary structure from circular
18 dichroism spectra: comparison of CONTIN, SELCON, and CDSSTR methods with an
19 expanded reference set. *Anal Biochem* 287:252–260
20
21

22
23 Vitali F, Henning A, Oberstrass FC, Hargous Y, Auweter SD, Erat M, Allain FH (2006)
24 Structure of the two most C-terminal RNA recognition motifs of PTB using segmental
25 isotope labeling. *EMBO J* 25:150–162
26
27

28
29 Wang X, Tanaka Hall TM (2001) Structural basis for recognition of AU-rich element
30 RNA by the HuD protein. *Nat Struct Biol* 8:141–145
31
32
33
34
35
36
37
38
39
40
41
42
43
44
45
46
47
48
49
50
51
52
53
54
55
56
57
58
59
60
61
62
63
64
65

Figure Legends

Figure 1. HuR protein. (a) Schematic domain organization of HuR and constructs used in this study. (b) Sequence alignment of HuR and its homologous HuD protein. Green, red and blue boxes highlight RRM1, RRM2 and RRM3 domains, respectively. HNS is also represented. Secondary structure elements are marked by blue arrows for β -strands and red coil symbols for α -helices based on the prediction using PSIPRED server. Phosphorylation sites of serines, which have been mutated in this study, are framed in yellow boxes. (c) Superposition between the crystal structure of HuR RRM1 (PDB entry 3HI9; Benoit et al. 2010) and the homology model of HuR RRM12 built as described in Materials and Methods. The RMSD for backbone atoms of HuR RRM1 domain in both structures is 0.583 Å. Side-chains of serine residues to be phosphorylated are included.

Figure 2. Far-UV (190-250 nm) CD spectra of different HuR domain constructs. RRM domains are represented as follows: RRM1 in solid line (—), RRM2 in dashed line (---), RRM12 in dotted line (····) and HuR FL protein in dash dotted line (- · -).

Figure 3. Far-UV (190-250 nm) CD spectra of RRM12 WT and its phosphomimetic mutants. RRM12 WT is shown in blue solid line (—); RRM12-S88A in green solid line (—); RRM12-S88D in green dashed line (---); RRM12-S100A in black solid line (—) and RRM12-S100D in black dash line (---); RRM12-S158A in red solid line (—) and RRM12-S158D in red dashed line (---).

Figure 4. SDS-PAGE electrophoresis of HuR RRM12 WT.

Line 1 stands for a HuR RRM12 WT sample devoid of DTT, whereas lines 2 and 3 correspond to protein samples previously incubated with 5 and 0.5 mM of DTT,

1
2
3
4
5
6
7
8
9
10
11
12
13
14
15
16
17
18
19
20
21
22
23
24
25
26
27
28
29
30
31
32
33
34
35
36
37
38
39
40
41
42
43
44
45
46
47
48
49
50
51
52
53
54
55
56
57
58
59
60
61
62
63
64
65

respectively, for 90 min before loading into the gel. In each line, 4 μg of HuR RRM12 WT was loaded onto an 18% SDS-PAGE gel. M: Pro-stain protein molecular weight marker (Intron Technologies Inc.).

Figure 5. Effect of Phosphomimetic Mutations on the Thermal Stability of HuR.

Unfolding thermal denaturation of HuR RRM species and their mutants was determined by DSF by following the fluorescent changes of SYPRO Orange. (a) RRM1 is represented in filled squares (■), RRM2 in filled circles (●) and RRM12 WT in open triangles (Δ). Ser-by-Asp substitutions are represented as follows: (b) RRM12 S88D (■); (c) RRM12 S158D (●); (d) RRM12 S100D (\blacktriangle). Fitting unfolding curves are represented by solid lines, and they are superimposed on experimental data. The melting points (T_m) of the transitions are marked by dashed lines.

Figure 6. Changes in the CD signal in the range of 260-275 nm region of the *c-fos* 11-mer RNA (5'AUUUUUAUUUU 3') spectrum during a titration with HuR RRM12 WT. Dissociation constant is also shown.

Table 1. Percentage of secondary structure for the different constructs of HuR RRM domains and mutant species.

Constructs	α-helix (%)	β-strand (%)	Turn (%)	Unstructured (%)*
RRM1	6.01 \pm 0.57	36.21 \pm 1.25	19.49 \pm 2.05	37.74 \pm 3.95
RRM2	10.84 \pm 0.22	34.11 \pm 0.65	19.13 \pm 0.90	30.81 \pm 1.61
RRM12 WT	5.72 \pm 0.77	39.67 \pm 4.39	21.22 \pm 1.80	33.03 \pm 3.10
RRM12 S88D	11.03 \pm 0.56	33.26 \pm 2.05	19.64 \pm 2.06	35.76 \pm 4.75
RRM12 S88A	5.87 \pm 0.44	39.00 \pm 1.68	20.42 \pm 1.41	34.25 \pm 2.40
RRM12 S100D	5.34 \pm 1.25	42.71 \pm 4.30	19.25 \pm 2.01	32.60 \pm 3.81
RRM12 S100A	3.18 \pm 0.39	40.88 \pm 1.34	21.23 \pm 1.15	34.78 \pm 2.90
RRM12 S158D	5.14 \pm 0.50	40.28 \pm 1.58	20.51 \pm 1.12	33.81 \pm 3.17
RRM12 S158A	5.16 \pm 0.34	39.79 \pm 1.40	21.04 \pm 1.65	33.75 \pm 3.29
HuR FL	9.18 \pm 1.79	34.95 \pm 0.83	20.01 \pm 2.39	35.23 \pm 4.74

*This makes reference to both disordered and flexible and ordered but non-regular structured parts of the protein.

1
2
3
4
5
6
7
8
9
10
11
12
13
14
15
16
17
18
19
20
21
22
23
24
25
26
27
28
29
30
31
32
33
34
35
36
37
38
39
40
41
42
43
44
45
46
47
48
49
50
51
52
53
54
55
56
57
58
59
60
61
62
63
64
65

Table 2. T_m values of HuR RRM domains and their phosphomimetic mutants, as calculated by CD and DSF

Constructs	T_m (K) by CD	T_m (K) by DSF
RRM1	335 ± 3	333 ± 1
RRM2	341 ± 2	339 ± 1
RRM12 WT	335 ± 2	332 ± 1
RRM12 S88D	336 ± 1	336 ± 2
RRM12 S88A	331 ± 1	330 ± 2
RRM12 S100D	334 ± 2	333 ± 1
RRM12 S100A	333 ± 1	330 ± 3
RRM12 S158D	330 ± 2	328 ± 3
RRM12 S158A	335 ± 1	330 ± 2

1
2
3
4
5
6
7
8
9
10
11
12
13
14 **Table 3. K_D values of the HuR RRM12 construct and its**
15 **phosphomimetic mutants, as calculated by CD titration**
16 **experiments with *c-fos* 11-mer RNA (5'AUUUUUAUUUU 3')**
17
18
19
20

Constructs	K_D (μM)
RRM12 WT	2.6 ± 0.2
RRM12 S88D	2.7 ± 0.2
RRM12 S100D	2.0 ± 0.1
RRM12 S158D	0.6 ± 0.3

21
22
23
24
25
26
27
28
29
30
31
32
33
34
35
36
37
38
39
40
41
42
43
44
45
46
47
48
49
50
51
52
53
54
55
56
57
58
59
60
61
62
63
64
65

Figure 1
[Click here to download high resolution image](#)

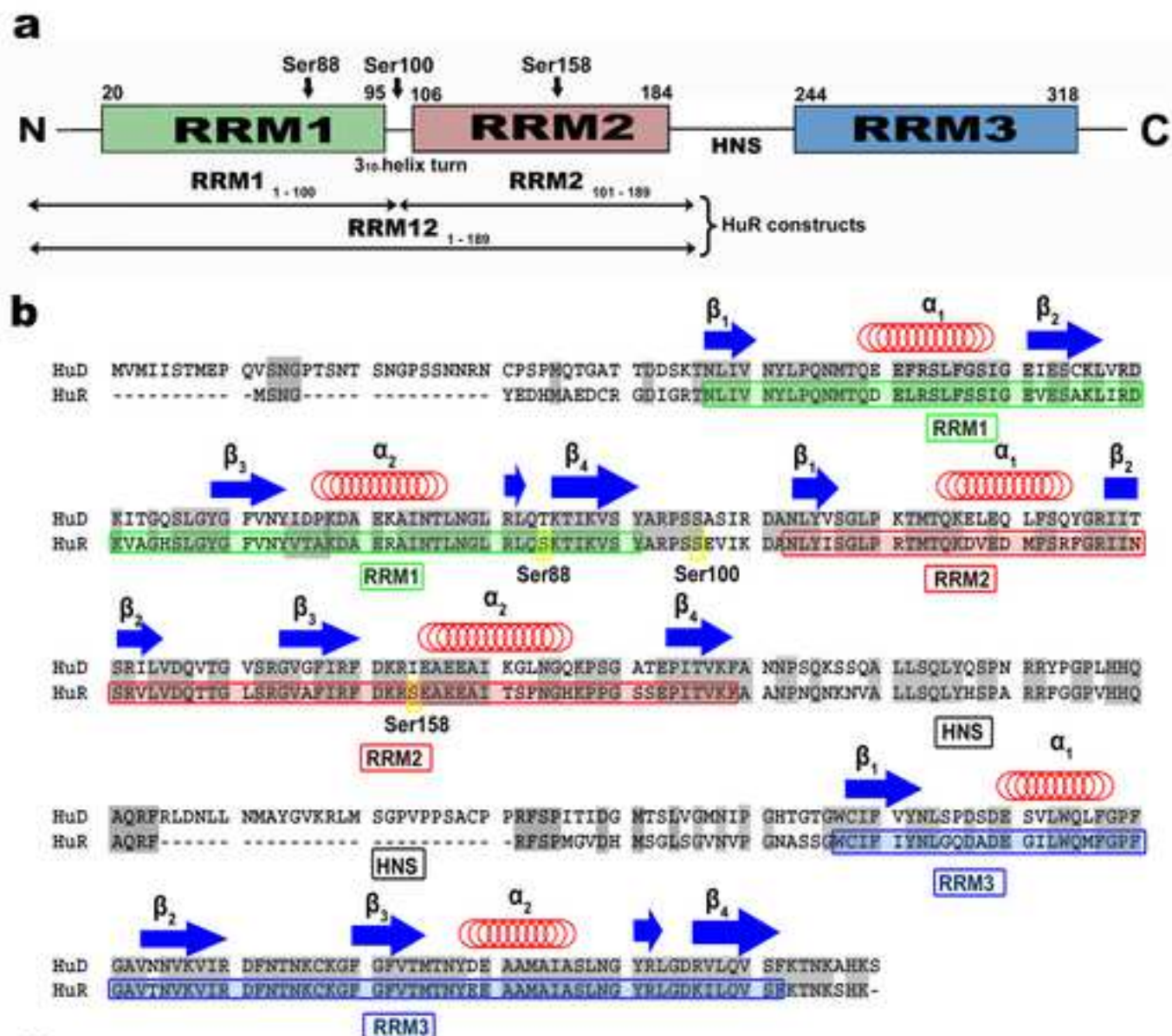


Figure 2
[Click here to download high resolution image](#)

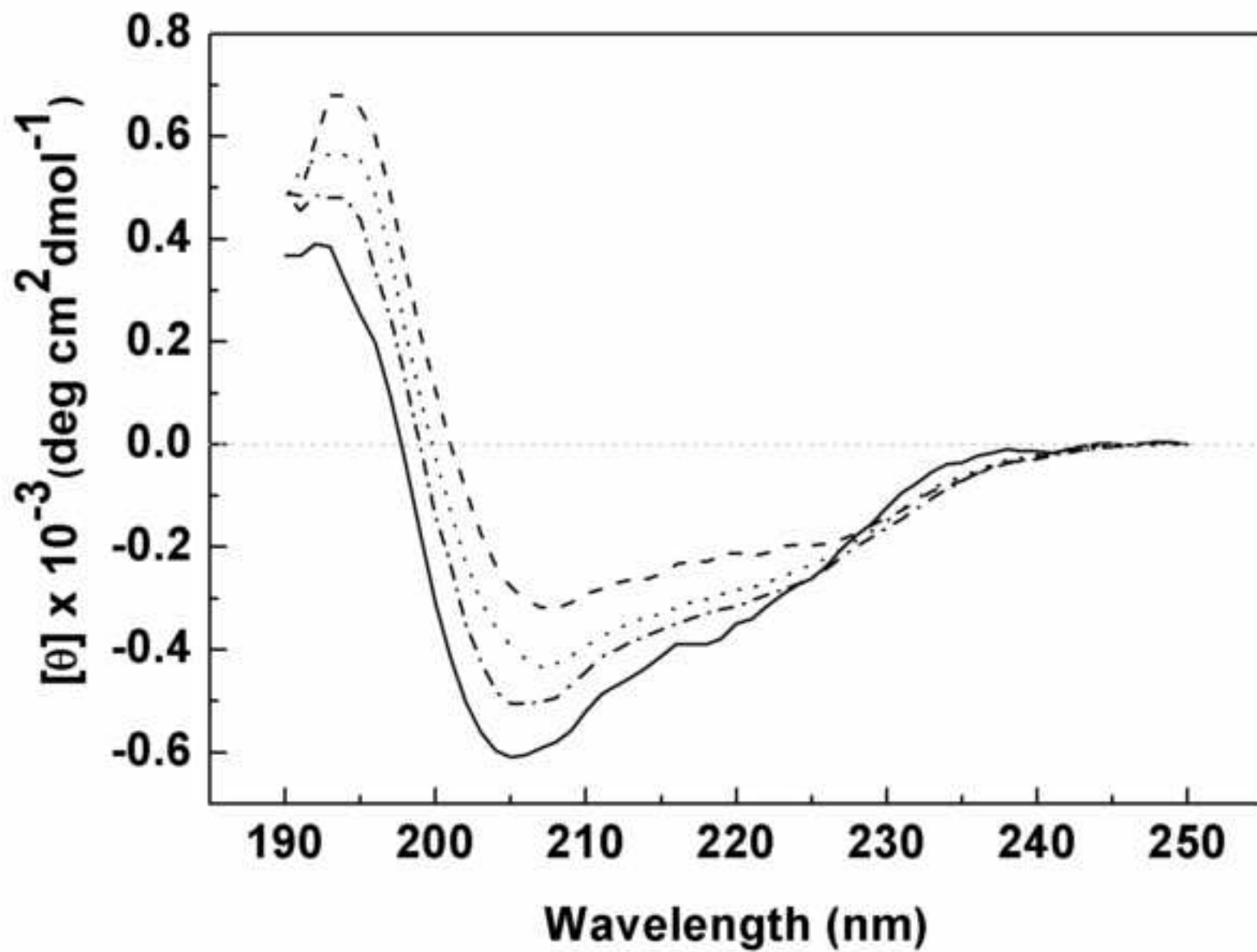


Figure 3
[Click here to download high resolution image](#)

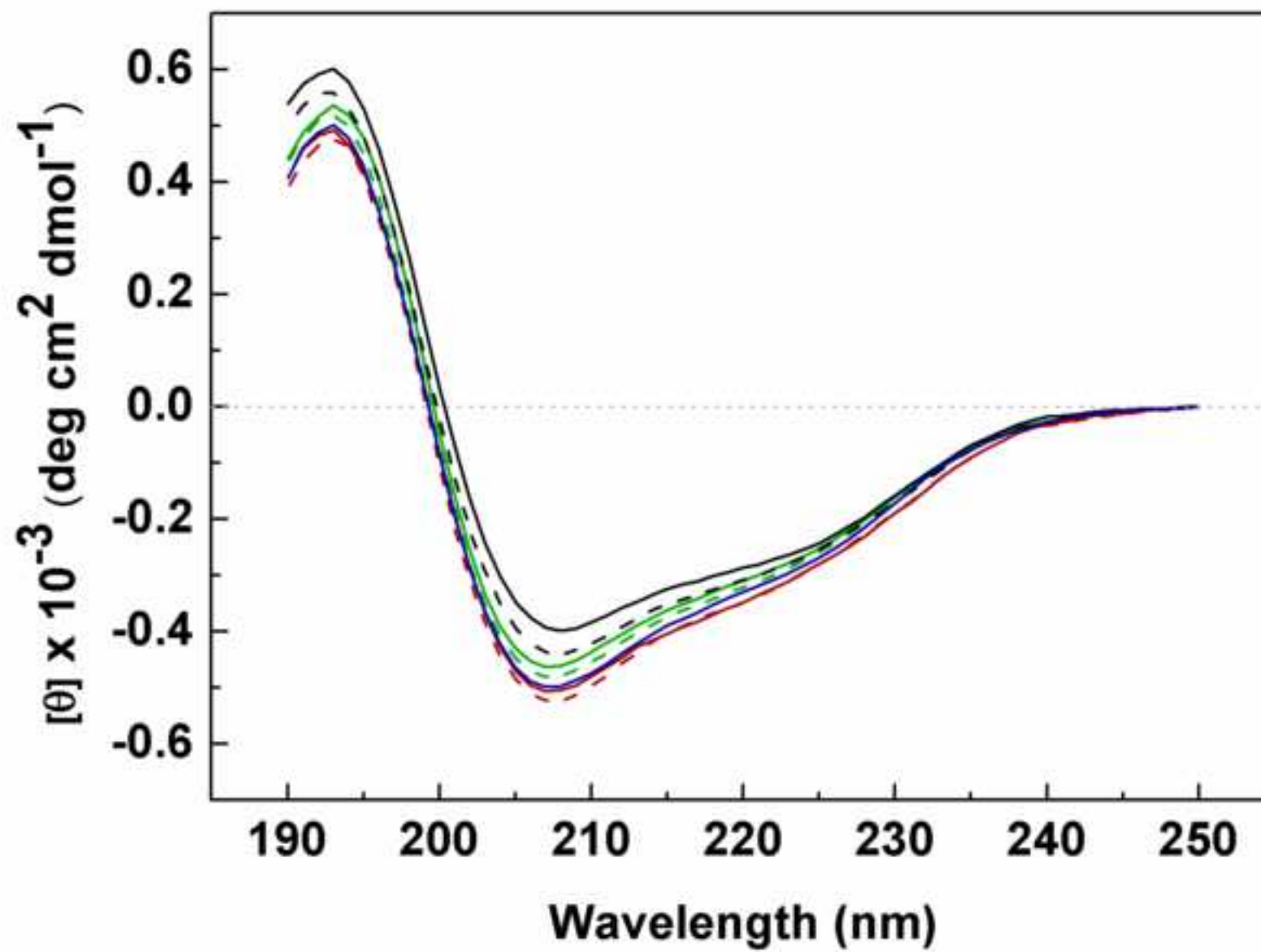


Figure 4
[Click here to download high resolution image](#)

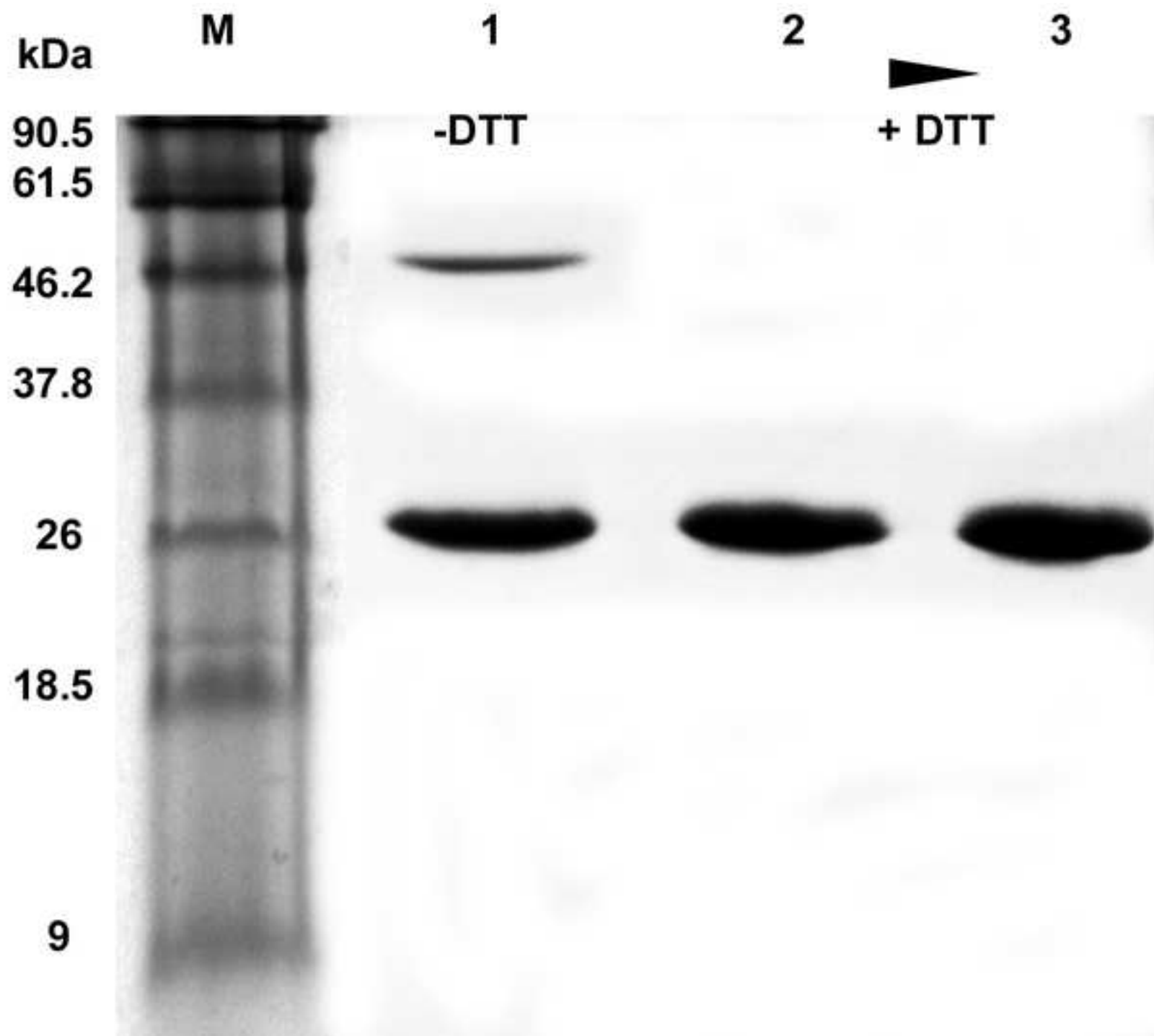


Figure 5
[Click here to download high resolution image](#)

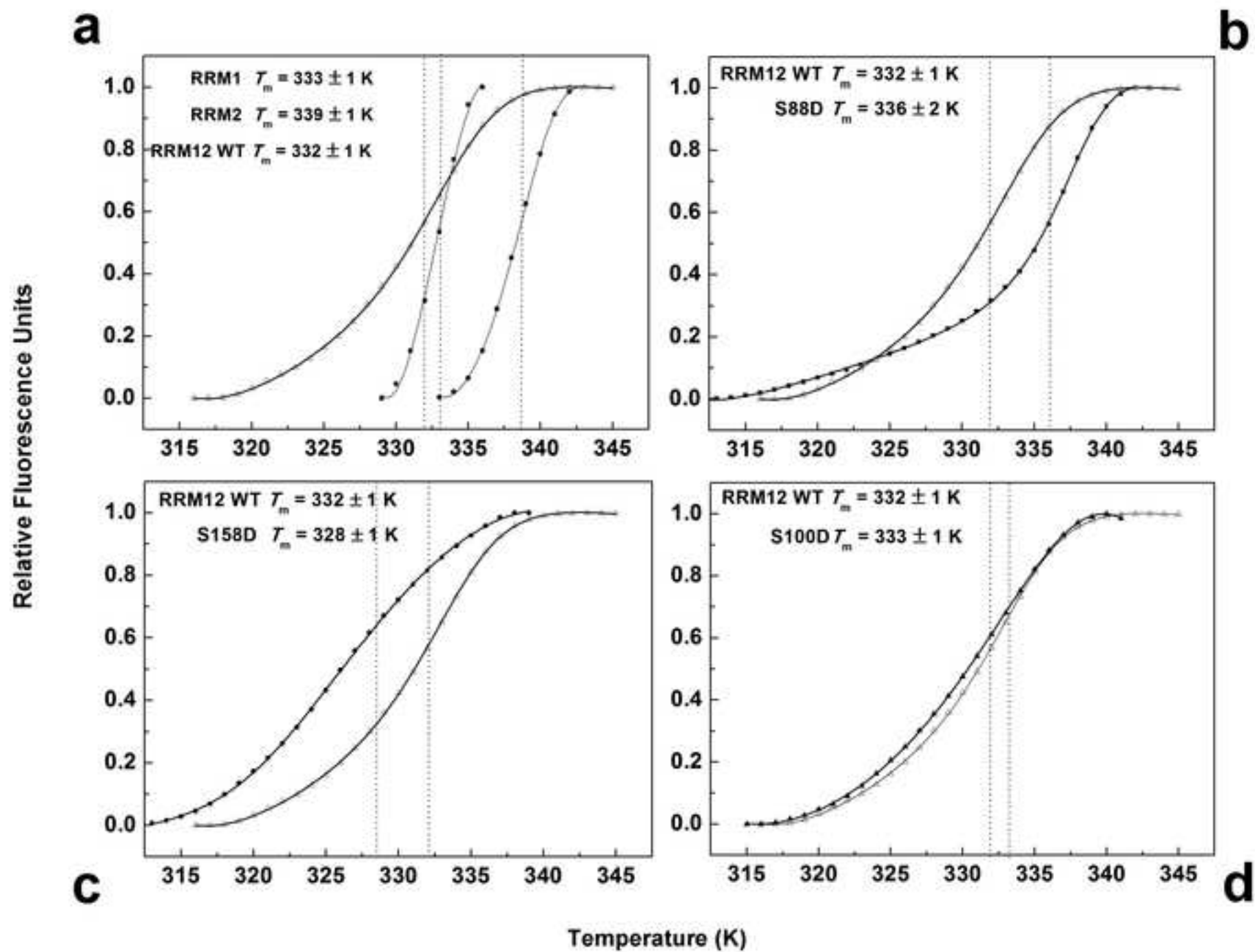


Figure 6
[Click here to download high resolution image](#)

